



First record and two new species of the genus *Subprotelater* Fleutiaux (Coleoptera, Elateridae, Subprotelaterinae) from Borneo

KÔICHI ARIMOTO^{1,*}, CLEMENT HET KALIANG², TAKAFUMI MIZUNO¹, PAULUS MELENG³, KEIKO KISHIMOTO-YAMADA⁴ & TAKAO ITIOKA^{1,5}

¹Graduate School of Global Environmental Studies, Kyoto University, Kyoto, 606–8501 Japan

✉ mizuno.takafumi.2x@kyoto-u.ac.jp; <https://orcid.org/0000-0001-7535-3052>

²Sarawak Forestry Corporation, Kuching, 93250 Malaysia

✉ hetk@sarawakforestry.com; <https://orcid.org/0000-0002-3241-6372>

³Research and Development Division, Forest Department Sarawak, Kuching, 93250 Malaysia

✉ paulusm@sarawak.gov.my; <https://orcid.org/0000-0003-3777-0597>

⁴Faculty of Advanced Science and Technology, Ryukoku University, Otsu, 520-2194 Japan

✉ kishimoto@rins.ryukoku.ac.jp; <https://orcid.org/0000-0003-3930-379X>

⁵Graduate School of Human and Environmental Studies, Kyoto University, Kyoto, 606–8501 Japan

✉ ichioka.takao.5m@kyoto-u.ac.jp; <https://orcid.org/0000-0002-8295-5657>

*Corresponding author: ✉ elateridbeetle@gmail.com; <https://orcid.org/0000-0002-8703-8073>

Abstract

The elaterid genus *Subprotelater*, the sole genus within the subfamily Subprotelaterinae, is known to include five species distributed across Japan, the Philippines, Singapore, and New Caledonia. In this study, we describe two new species, *Subprotelater lambirensis* sp. nov. and *Subprotelater miriensis* sp. nov., from Sarawak, Borneo, Malaysia, marking the first record of this genus in Malaysia. Additionally, we summarize information from previous reports on the known species and present an identification key.

Key words: elaterid beetles, Malaysia, new species, Oriental region, Sarawak

Introduction

The genus *Subprotelater* Fleutiaux, 1916, was established based on *Subprotelater bakeri* Fleutiaux, 1916, originally classified within the family Melasidae Fleming, 1821 (=subfamily Melasinae, family Eucnemidae Eschscholtz, 1829) based on the antennal grooves on the prothorax. In 1920, Fleutiaux placed the genus in the subfamily Subprotelaterinae within Melasidae. Subsequently, Cobos (1959) proposed transferring *Subprotelater* to the family Elateridae, citing its visible labrum and general body structure. Nakane (1987a) further suggested excluding the genus from Eucnemidae. Muona (1987), after examining the type species, supported its placement in Elateridae but raised questions about its systematic position within the family. Costa *et al.* (2010) and Kundrata *et al.* (2019) upheld this classification, treating Subprotelaterinae as a subfamily of Elateridae. The subfamily is made up of a single genus with five species: *S. bakeri* (described from the Philippines), *Subprotelater guttatus* Fleutiaux, 1919 (Singapore), *Subprotelater hisamatsui* Nakane, 1987 (Japan), *Subprotelater japonicus* Nakane and Hisamatsu, 1991 (Japan), and *Subprotelater williamsi* Van Zwaluwenberg, 1941 (New Caledonia). Among these, three species have no additional records beyond their original descriptions, whereas the two Japanese species have been frequently reported (Yamaji, 1998; Suzuki, 2002, 2003, 2024; Makihara and Ôhira, 2006; Watanabe, 2008; Takahashi, 2010; Noto, 2024). Lawrence *et al.* (2000 onwards) provided generic morphological descriptions of the genus, including details of the entire body and mouthparts. Watanabe (2008) added morphological features of *S. japonicus*, including an image of the male aedeagus. However, information useful for distinguishing species, particularly genitalia structures, has not been updated in recent years. Consequently, identifying *Subprotelater* species remains challenging, relying primarily on body color and markings rather than detailed structural features. Since the 1990s, field surveys

in Lambir Hills National Park, Sarawak, Malaysia, have collected insect specimens to investigate the biodiversity of Borneo. During these surveys, additional *Subprotelater* specimens were discovered, marking the first record of this genus in Malaysia. This study examines these specimens to identify diagnostic features for species identification and describes two new species, including detailed characteristics of their mouthparts and genitalia. Additionally, we consolidate information from previous reports on known species and provide an identification key for the genus.

Material

The specimens were collected using traps in the southern region of Lambir Hills National Park (4°12' N, 114°02' E; 50–250 m above sea level), an area predominantly covered by primary lowland dipterocarp forest in northwestern Malaysian Borneo. Ultraviolet light traps were deployed at heights of 1 m, 17 m, and 35 m within a tree tower, while flight interception traps (FITs) were set in the canopy at heights of 30–50 m using a canopy crane. The examined specimens are housed at the Kuching Insectarium of the Forest Department Sarawak (KIFDS; Kuching, Sarawak, Malaysia), managed by the Research and Development Division of the Forest Department Sarawak, which is one of the Sarawak government agencies. The unique identifier numbers for the specimens are AA2737–AA2742.

Methods

The methods for specimen observation, photography, dissection, and deposition of dissected parts followed the protocols outlined by Arimoto (2023). After publication, labels containing bibliographic information will be attached to all examined specimens. Digital images of photographs and maps were edited and enhanced using Adobe Photoshop v24.6.0 (Adobe, San Jose, CA, USA). The generic classification of the subfamily Subprotelaterinae follows Kundrata *et al.* (2019). Morphological nomenclature primarily adheres to the systems proposed by Costa *et al.* (2010) and Lawrence *et al.* (2021), with supplementary references to the frameworks of Calder (1996) and Douglas (2017).

Measurements and indices

Measurements are shown in millimeters. The following abbreviations are used:

BL Body length from head frontal margin to elytral apices

BW The maximum body width

MAE The maximum distance across the eyes in dorsal view

MBE The minimum distance between the eyes in dorsal view

OI Ocular index: $MAE/MBE \times 100$

PL The maximum pronotum length including hind angles

PML Length of the midline of the pronotum, equivalent to the minimum pronotum length in this study

PW The maximum pronotum width including hind angles

PAW The pronotum width between the anterior angles, equivalent to the minimum pronotum width in this study

PLI Pronotum length index: $PL/PW \times 100$

PWI Pronotum width index: $PW/PAW \times 100$

EL The maximum elytron length

EW The maximum elytron width

EI Elytra index: $EL/EW \times 100$

BI Body index: $EL/PL \times 100$

Taxonomy

Genus *Subprotelater* Fleutiaux, 1916

Subprotelater Fleutiaux, 1916: (original description; type species: *Subprotelater bakeri*).

Diagnosis. This genus is distinguished from the other elaterid genera by the deep antennal grooves between pronotum and hypomeron and the deeply grooved pronotosternal sutures receiving pro-tarsi.

Included species. Seven species: *S. bakeri* Fleutiaux, 1916 (Philippines: Luzon), *S. guttatus* Fleutiaux, 1919 (Singapore), *S. hisamatsui* Nakane, 1987 (Japan: Ogasawara Islands), *S. japonicus* Nakane and Hisamatsu, 1991 (Japan: Honshu), *S. lambirensis* Arimoto, **sp. nov.** (Malaysia: Borneo), *S. miriensis* Arimoto, **sp. nov.** (Malaysia: Borneo), *S. williamsi* Van Zwaluwenberg, 1941 (New Caledonia).

Remarks. Nakane (1987b) reported a specimen from Honshu, Japan as *Subprotelater* sp. Nakane (1991) described the species as new, *S. japonicus*, with the authority as “Nakane et Hisamatsu”.

Lawrence *et al.* (2000 onwards) showed a species from Australia without assigning it a species name.

Subprotelater hisamatsui was proposed as a junior synonym of *S. bakeri* based on a comparison of a dorsal-view photograph of the holotype of *S. bakeri* (Suzuki, 2003). However, a detailed direct comparison between these species has not been conducted. Suzuki (2022, 2024) adhered to this suggestion and treated species from the Ogasawara Islands, Japan, as *S. bakeri*.

Makihara and Ôhira (2006) examined a specimen from Babeldaob Island, Palau, but did not assign it to a specific species. Suzuki (2024) subsequently treated this specimen as *S. bakeri*, although it has not been re-examined.

Ecology. The two new species, *Subprotelater lambirensis* and *Subprotelater miriensis*, were collected in primary lowland dipterocarp forest using FITs at heights of 30–50 m and ultraviolet light traps at 17m and 35 m, respectively (this study). *Subprotelater hisamatsui* was collected using Malaise traps (Suzuki, 2003), black light traps (Makihara and Ôhira, 2006), and sticky traps placed on branches of trees, particularly *Schima mertensiana* (Suzuki, 2024). *Subprotelater japonicus* has been collected in various settings, for example, on rotting wood with bracket fungi likely belonging to the family Polyporaceae (Nakane, 1987b) and on the decaying wood of *Quercus gilva* (Arimoto, 2019), and using different methods such as FITs (Watanabe, 2008) and vegetation beating (Takahashi, 2010; Noto, 2024). This species was found from the lowland forest to natural forest consisting mainly of beech and mizunara oak around 800m (Watanabe, 2008; Takahashi, 2010). The northernmost distribution of this species, and of the genus, is approximately 39.6° N, 141.1° E (Takahashi, 2010). *Subprotelater williamsi* was collected while being on the bark of the weeping paperbark tree (*Melaleuca leucodendron*) in lowland areas (Van Zwaluwenberg, 1941).

Key to the species of the genus *Subprotelater*

1. Elytron with narrow yellow longitudinal stripe near apical mesial edge 2
- Elytron without narrow yellow longitudinal stripe near apical mesial edge 3
2. Elytron with yellow straight transverse spot posteriorly *S. bakeri* Fleutiaux, 1916
- Elytron with yellow curved transverse spot posteriorly *S. hisamatsui* Nakane, 1987
3. Elytron with four yellow spots 4
- Elytron with three yellow spots *S. japonicus* Nakane and Hisamatsu, 1991
4. Body and antennae black; median longitudinal carina of pronotal posterior angles distinct 5
- Body brown and antennae orange; median longitudinal carina of pronotal posterior angles vestigial *S. miriensis* Arimoto, **sp. nov.**
5. Setae yellowish; pronotum without impressions before the middle 6
- Setae black on dorsal side of the body and greyish on its underside; pronotum with two vague impressions on either side before the middle *S. williamsi* Van Zwaluwenberg, 1941
6. Prothorax punctures small; interspaces between punctures generally larger than puncture diameter; metepisternum narrower than width of elytral epipleuron *S. lambirensis* Arimoto, **sp. nov.**
- Pronotum with large and umbilicate punctures; prosternum and hypomeron with very tight and large punctures; metepisternum width equal to width of elytral epipleuron *S. guttatus* Fleutiaux, 1919

Subprotelater lambirensis Arimoto, sp. nov.

(Figures 1–3)

Type material. Holotype. Male (AA2737), Malaysia, Sarawak, Miri, Lambir Hills National Park, 22 IX 2010, Keiko Kishimoto-Yamada and Takao Itioka leg., by FIT in the canopy.

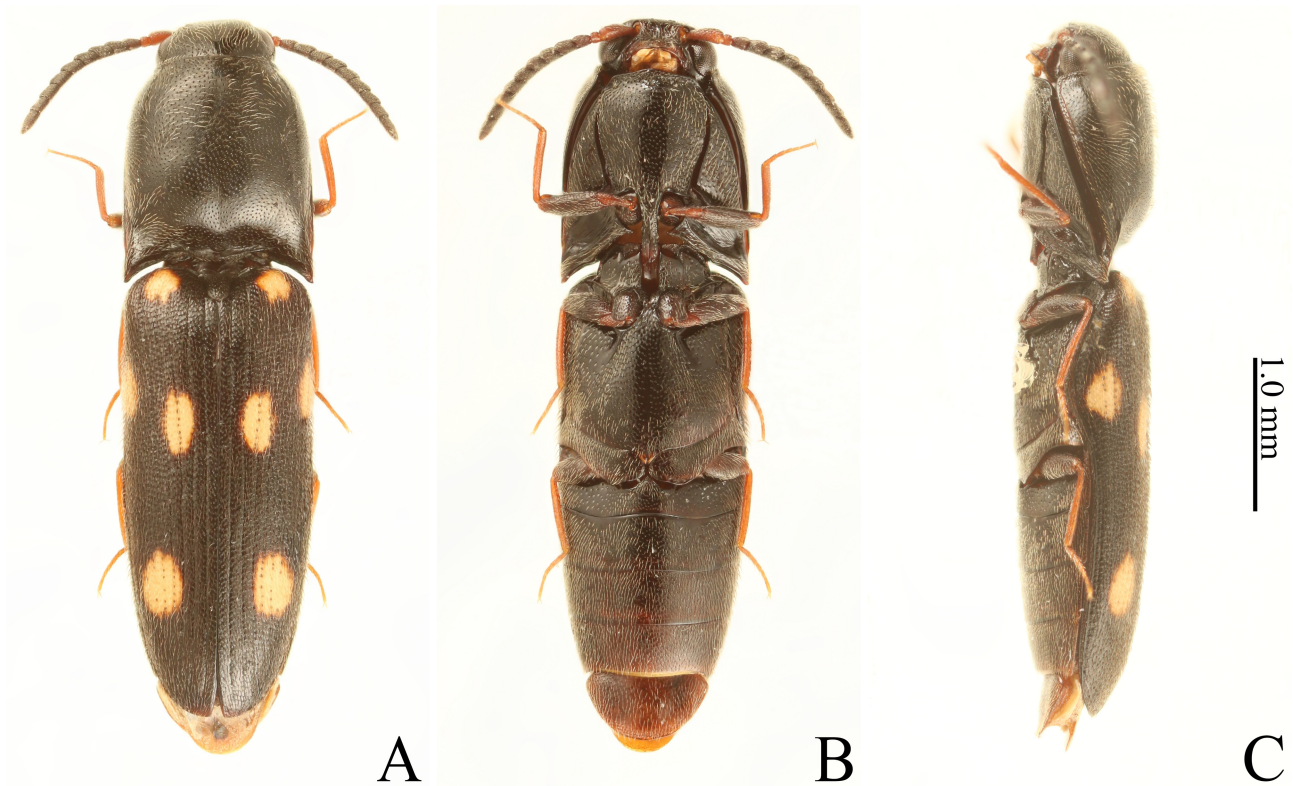


FIGURE 1. *Subprotelater lambirensis* Arimoto, sp. nov., holotype, male (AA2737). A: Habitus, dorsal side; B: habitus, ventral side; C: habitus, left side.

Male. Diagnosis. This species is characterized by the following features: punctures small; interspaces between punctures generally larger than puncture diameter; body black; elytron with four sub-circular yellow spots; antennomeres I and II dark red; antennomeres III–IX black; legs dark red but coxae and femurs black tinged with red; setae yellow brown; pronotum $1.2 \times$ longer than wide; prosternal process $1.8 \times$ longer than procoxal cavity length in ventral view; mesal posterior angle of hypomerion strongly protruding; posterior part of scutellar shield not visible in lateral view; elytron $4.8 \times$ longer than wide, $2.0 \times$ longer than pronotal length; metepisternum narrower than width of elytral epipleuron; basal struts $0.15 \times$ total length of median lobe; apices of parameres roundly truncate.

Measurements. BL: 4.52, BW: 1.25, MAE: 0.78, MBE: 0.53, OI: 146, PL: 1.48, PML: 1.31, PW: 1.23, PAW: 0.79, PLI: 120, PWI: 156, EL: 2.92, EW: 0.61, EI: 479, BI: 198.

Description. Body (Fig. 1) elongate; surface generally smooth, shining, but rough on depression of hypomerion for reception of pro-femur and tibia; punctures small; depressions of hypomerion for reception of proleg and of mesepimeron and metasternum for reception of midleg without punctures; interspaces between punctures generally larger than puncture diameter. Color. Body black. Elytron with four sub-circular yellow spots, of which one spot medially on humerus, two spots side-by-side on anterior 1/3, and one spot medially on posterior 1/3. Pronotal posterior lateral apices, posterior external edge of antennal groove of hypomerion, apical part of prosternal process, distal edge of elytron, posterior margins of metasternum and metacoxal plates and posterior part of abdomen tinged with red. Mouthparts yellowish with labrum and mandibles dark red; antennomeres I and II dark red; III–IX black; legs dark red but coxae and femurs black tinged with red. Body covered with yellow brown setae (Fig. 1A, B).

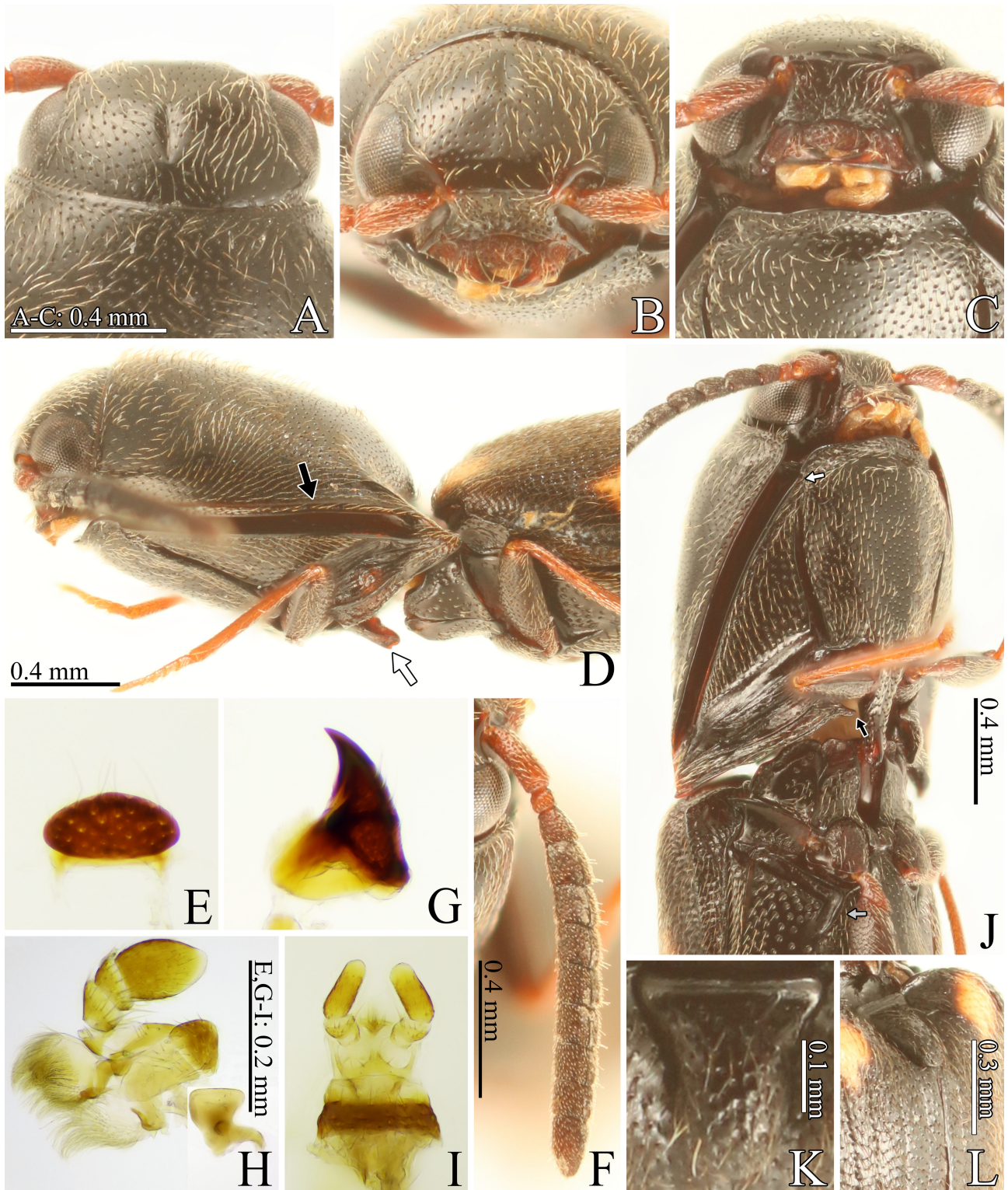


FIGURE 2. *Subprotelater lambirensis* Arimoto, **sp. nov.**, holotype, male (AA2737). A: Head, dorsal view; B: head, anterior view; C: head, anteroventral view; D: head, prothorax and mesothorax, lateral view (black arrow: lateral carina along antennal groove; white arrow: pointed subapical tooth); E: labrum; F: right antenna; G: right mandible; H: right maxilla; I: labium; J: prothorax and mesothorax, ventrolateral view (white arrow: anterior angle of hypomeron sharply pointed, black arrow: mesal posterior angle of hypomeron strongly and sharply protruding, gray arrow: metasternum carinate ahead of depression for reception of mid-tibia and ventrad of depression for reception of mid-tarsi); K: scutellar shield; L: scutellum and elytra, dorsolateral view.

Head. Frontal margin broadly rounded in dorsal view (Fig. 2A); frons distinctly depressed mesally and longitudinally (Fig. 2A, B); supra-antennal carina absent (Fig. 2B, C); frontoclypeal region most protruding between antennal sockets (Fig. 2D), grooved between eyes and mandibles (Fig. 2C); the grooves receive basal two antennomeres, opened posteriorly. Eyes $0.15 \times$ longer than interocular distance in dorsal view. Mouthparts directed ventrally (Fig. 2D). Labrum semioval (Fig. 2E), $0.5 \times$ longer than wide. Antennae extended beyond half-length of pronotum and not reaching pronotal posterior lateral apices by antennomere XI (Fig. 1A); relative antennomere lengths: $II < III < IV - X < XI < I$ (Fig. 2F); antennomere I elongate and curved cylindrical; II short cylindrical, $0.9 \times$ longer than wide; III trapezoidal, $1.2 \times$ longer than wide, $1.9 \times$ longer than II; IV–X parallelogram, weakly rounded distally, 1.1 – $1.2 \times$ longer than wide; IV $1.2 \times$ longer than III, $0.8 \times$ longer than II–III combined; V $0.95 \times$ longer than IV; XI bullet shaped, $1.8 \times$ longer than wide, $1.45 \times$ longer than X; each antennomeres with a longitudinal carina distally; the carinae on VIII–X not reaching their anterior edge, and carina on XI short. Mandibles unidentate (Fig. 2G); penicillus short, formed by brush of short setae; dorsal sinuous carina developed; with setae of various lengths on outside of the carina; outside concave basally (Fig. 2C). Maxilla (Fig. 2H): cardo constricted posteriorly; basistipe triangular; mediostipe bullet-shaped; galea short, brush-like; lacinia short, brush-like; palpomeres short and broad; palpomeres II–III shorter than wide; palpomere IV fusiform, $1.4 \times$ longer than wide. Labium (Fig. 2I): mentum wide trapezoidal, with long setae; prementum with cluster of short setae medially; apical palpomere cylindrical.

Prothorax widened posteriad but almost parallel-sided on posterior half, widest on posterior $1/5$, and then weakly narrowed ahead of posterior angles (Fig. 1A). Antennal grooves between pronotum and hypomeron deep and opened anteriorly, not reaching posterior lateral apices of prothorax, visible in lateral view (Fig. 2D); sides of antennal grooves carinate. Pronotum sub-hexagonal, $1.2 \times$ longer than wide, roundly convex, tallest posterior to the center (Fig. 2D), with median longitudinal depression posteriorly; each lateral carina extending from posterior angles along antennal grooves (Fig. 2D: black arrow), not reaching anterior angles; anterior angles obtuse (Fig. 2A); anterior edge straight in dorsal view (Fig. 2A); posterior angles extending posteriad, moderately broad, uncarinate; posterior edge without sublateral incision near each hind angle, lobated and protruding medially. Hypomeron depressed for reception of pro-femur and tibia, carinate behind the depression; anterior angle sharply pointed (Fig. 2J: white arrow); posterior edge broadly rounded mesally and weakly emarginate near distal posterior angle; mesal posterior angle strongly and sharply protruding (Fig. 2J: black arrow). Pronotosternal sutures (Fig. 1B) deeply grooved to receive pro-tarsi; tarsal groove opened posteriorly and connected to hypomeron depression for reception of pro-femur and tibia (Fig. 2J), becoming shallower anteriorly, not reaching anterior edges of hypomeron and prosternum. Prosternum: anterior edge carinate, roundly projecting medially, depressed posterior to prosternal lobe; prosternal lobe short, not reaching the level of anterior edge of prothorax (Fig. 2D). Prosternal process $1.8 \times$ longer than procoxal cavity length, depressed between procoxae, strongly curved dorsad behind procoxae (Fig. 2D); dorsal margin broadly rounded but with shallow concave medially in lateral view (Fig. 2D); ventral lobe almost parallel sided and gradually narrowed near apex in ventral view, with median longitudinal carina on posterior $1/3$ (Fig. 1C); the carina forming pointed subapical tooth (Fig. 2D: white arrow); ventral margin rounded inward anteriorly and straight posteriorly in lateral view (Fig. 2D); ventral apex reaching dorsal apex; apex rounded in ventral and lateral views (Figs. 1C, 2D). Scutellar shield strongly inclined anterior-downwards (Fig. 1A), tongue-shaped in anterodorsal view (Fig. 2K), narrowed posteriad but almost parallel-sided around its half-length, $1.1 \times$ longer than wide, convex (Fig. 2L); anterior part protruding anteriorly (Figs. 1A, 2L); posterior part not visible in lateral view (Fig. 2D); anterior angles rounded; anterior edge straight; apex rounded. Mesosternum (Fig. 3A): anterior edge straight but sinuate laterally, lobate on each side; mesosternal cavity floor without median band of setae; mesosternal cavity almost parallel-sided in ventral view; borders of mesosternal cavity in lateral view rounded anteriorly, straight medially and then curved ventrad obtusely (Fig. 2D); mesosternal process between mesocoxae lower than mesocoxae, not visible in lateral view (Fig. 2D); posterior edge $0.2 \times$ wider than total width of mesosternum, almost straight (Fig. 3A); mesosternum and metasternum connate medially (Fig. 2J). Mesepisternum excavate anteriorly (Fig. 2J). Mesepimeron depressed for reception of mid-femur (Fig. 2J). Mesocoxal cavity closed to mesepisternum by mesosternum and mesepimeron (Fig. 2J). Elytron $4.8 \times$ longer than wide, $2.0 \times$ longer than pronotal length, parallel-sided but narrowed from posterior $1/2$, rounded apically, broadly convex but plane medially (Fig. 1C), with striae. Elytral apices not meeting at midline (Fig. 1A). Hind wings (Fig. 3B) fully developed, without veins CuA_1 and CuA_{3+4} ; RA_{3+4} vestigial (Fig. 3B: white arrow); r_4 translucent; mediomedial-cross vein between MP_{1+2} and MP_{3+4} translucent (Fig. 3B: black arrow); mediocubital cross-vein between MP_{3+4} and CuA_2 absent (Fig. 3B: grey arrow); AA_3 vestigial; radial cell $4.0 \times$ longer than wide. Metepisternum narrower than width of elytral epipleuron (Fig. 2J).

Metasternum depressed for reception of mid-tibia and tarsi, carinate ahead of depression for reception of mid-tibia and ventrad of depression for reception of mid-tarsi (Fig. 2J: grey arrow), sulcate medially and ahead of metacoxal cavities (Fig. 1B). Metacoxal plate narrowed medially; lateral edge distinctly longer than width of metepisternum; lateral anterior angle rounded; lateral posterior angle broadly pointed (Fig. 3C: arrow). Tibiae with a pair of simple spurs (Fig. 3D: arrow); relative tarsomere lengths: $IV < III < II < I < V$ (Fig. 3D); tarsi and claws simple.

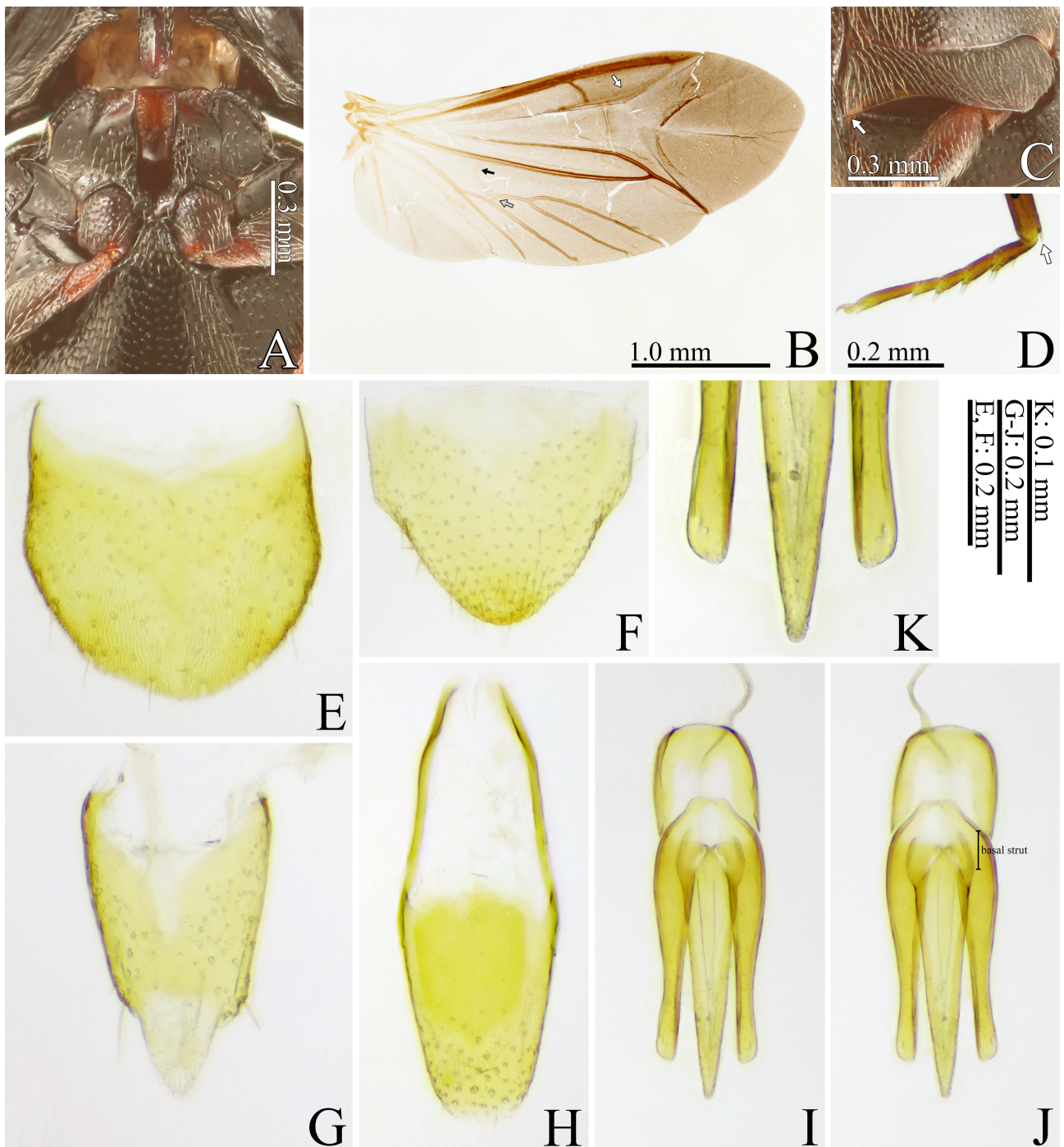


FIGURE 3. *Subprotelater lambirensis* Arimoto, **sp. nov.**, holotype, male (AA2737). A: Mesothorax and metathorax, ventral side; B: right hind wing (white arrow: vein RA_{3+4} vestigial, black arrow: mediomedial cross-vein between MP_{1+2} and MP_{3+4} translucent, gray arrow: mediocubital cross-vein between MP_{3+4} and CuA_2 absent); C: metacoxal plate (arrow: lateral posterior angle broadly pointed); D: left mid tarsus, lateral side (arrow: tibiae with a pair of simple spurs); E: tergite VIII; F: sternite VIII; G: tergites IX–X; H: sternite IX; I: aedeagus, dorsal side; J: aedeagus, ventral side; K: apical part of aedeagus, dorsal view.

Abdomen. Ventricle V semicircular, broadly rounded apically (Fig. 1B), $0.55 \times$ longer than wide. Tergites and sternites VIII–X yellow. Tergite VIII (Fig. 3E) as long as wide, almost parallel-sided basally but weakly sinuate, broadly rounded apically. Sternite VIII (Fig. 3F) triangular, abruptly narrowed at its half-length, shorter than wide; apex rounded. Tergite IX (Fig. 3G) trapezoidal; anterior edge widely emarginate; median translucent area reaching tergite X. Tergite X (Fig. 3G) curved triangular, widely emarginate anteriorly, rounded apically, $1.2 \times$ longer than wide, $0.45 \times$ length of tergite IX. Sternite IX (Fig. 3H) elongate oval, widest at its half-length, broadly rounded apically. Aedeagus (Fig. 3I, J) yellow, elongate. Phallobase $0.3 \times$ total length of aedeagus, $1.1 \times$ longer than wide. Median lobe gradually tapering to apex, exceeding apices of parameres by its apex; basal struts $0.15 \times$ total length of median lobe. Parameres separated ventrally; apical parts without lateral subapical barbs, roundly truncate apically, without setae (probably due to damage).

Female. Unknown.

Etymology. The specific epithet derives from Lambir Hills National Park, the type locality.

Distribution. Malaysia (Borneo).

Ecology. The life history and ecology of this species remain unknown, except that the holotype was collected via FIT in the canopy.

Subprotelater miriensis Arimoto, sp. nov.

(Figures 4–6)

Type material. Malaysia, Sarawak, Miri, Lambir Hills National Park, by ultraviolet light traps. **Holotype.** Male (AA2739), 17 m, 23–24 VIII 1998. **Paratypes.** 1 male (AA2738), 17 m, 14–15 XII 1996; 1 male (AA2740), 35 m, 18–19 XII 1998; 1 male (AA2741), 17 m, 17–18 V 1999; 1 male (AA2742), 35 m, 15–16 II 2002.

Male. Diagnosis. This species is characterized by the following features: punctures large and umbilicate; interspaces between punctures generally shorter than puncture diameter; body brown; antennae and legs orange; elytron with four sub-circular yellow spots; setae yellow; pronotum $1.3 \times$ longer than wide; prosternal process 2.0 – $2.3 \times$ longer than procoxal cavity length in ventral view; mesal posterior angle of hypomerion obtuse, not protruding; posterior part of scutellar shield visible in lateral view; elytron 5.2 – $5.5 \times$ longer than wide, 2.0 – $2.2 \times$ longer than pronotal length; metepisternum narrower than width of elytral epipleuron; basal struts $0.3 \times$ total length of median lobe; apices of parameres tapering to apex.

Measurements (5 specimens; holotype in parentheses). BL: 4.61–6.13 (4.61), BW: 1.11–1.54 (1.11), MAE: 0.90–1.11 (0.90), MBE: 0.54–0.66 (0.54), OI: 160–171 (169), PL: 1.41–1.99 (1.41), PML: 1.28–1.75 (1.28), PW: 1.10–1.56 (1.10), PAW: 0.87–1.12 (0.87), PLI: 128–129 (129), PWI: 126–146 (126), EL: 3.01–4.02 (3.01), EW: 0.55–0.75 (0.55), EI: 521–545 (545), BI: 197–216 (213).

Description. Body (Fig. 4) elongate; surface generally smooth, shining but rough on depression of hypomerion for reception of pro-femur and tibia and on depressions of mesepimeron and metasternum for reception of mid-leg; punctures large and umbilicate, but on elytra small; depressions of hypomerion for reception of proleg and of mesepimeron and metasternum for reception of midleg without punctures; interspaces between punctures generally shorter than puncture diameter, but on metasternum, elytra and abdominal ventrites larger than puncture diameter and partly shorter than puncture diameter. Color. Body brown. Elytron with four sub-circular yellow spots, of which one spot medially on humerus, two spots side-by-side on anterior 1/3, and one spot medially on posterior 1/3. External edge of mandibles, mesal edge of antennal groove of hypomerion, sides of tarsal groove of pronotosternal sutures, external edge of scutellar shield, metasternal carina ventrad of depression for reception of mid-tarsi, striae and distal edge of elytron, and posterior edge of each abdominal ventrite blackish. Mouthparts yellowish with labrum and mandibles red-brown; antennae and legs orange with yellow tarsi. Body covered with yellow setae (Fig. 4).

Head. Frontal margin broadly rounded in dorsal view (Fig. 5A); frons weakly depressed mesally (Fig. 5A, B); supra-antennal carina absent (Fig. 5B, C); frontoclypeal region most protruding between antennal sockets (Fig. 5D), grooved between eyes and mandibles (Fig. 5C); the grooves receive basal two antennomeres, opened posteriorly. Eyes 0.25 – $0.35 \times$ longer than interocular distance in dorsal view. Mouthparts directed ventrally (Fig. 5D). Labrum elliptical, anterior edge more tapered (Fig. 5E), $0.5 \times$ longer than wide. Antennae extended beyond half-length of pronotum and not reaching pronotal posterior lateral apices by antennomere XI (Fig. 4A, B); relative antennomere

lengths: II < III < IV–X < XI < I (Fig. 5F); antennomere I elongate and curved cylindrical; II short cylindrical, 0.8–0.85 × longer than wide; III trapezoidal, 1.1–1.4 × longer than wide, 2.0–2.4 × longer than II; IV–X parallelogram, weakly rounded distally, 1.1–1.3 × longer than wide; IV 1.1–1.2 × longer than III, 0.75–0.9 × longer than II–III combined; V 1.0–1.05 × longer than IV; XI bullet shaped, 1.7–2.1 × longer than wide, 1.3–1.5 × longer than X; each I–X with longitudinal carina distally; carinae on VI–X not reaching to their anterior edge. Mandibles unidentate (Fig. 5G); penicillus short, formed by brush of short setae; dorsal sinuous carina developed; with setae of various lengths on outside of the carina; outside concave basally (Fig. 5C). Maxilla (Fig. 5H): cardo constricted posteriorly; basistipe triangular; mediostipe rectangular; galea short, brush-like; lacinia short, brush-like; palpomeres short and broad; palpomeres II–III shorter than wide; palpomere IV fusiform, 1.2–1.3 × longer than wide. Labium (Fig. 5I): mentum wide trapezoidal, with long setae; prementum with cluster of short setae medially; apical palpomere subcylindrical.

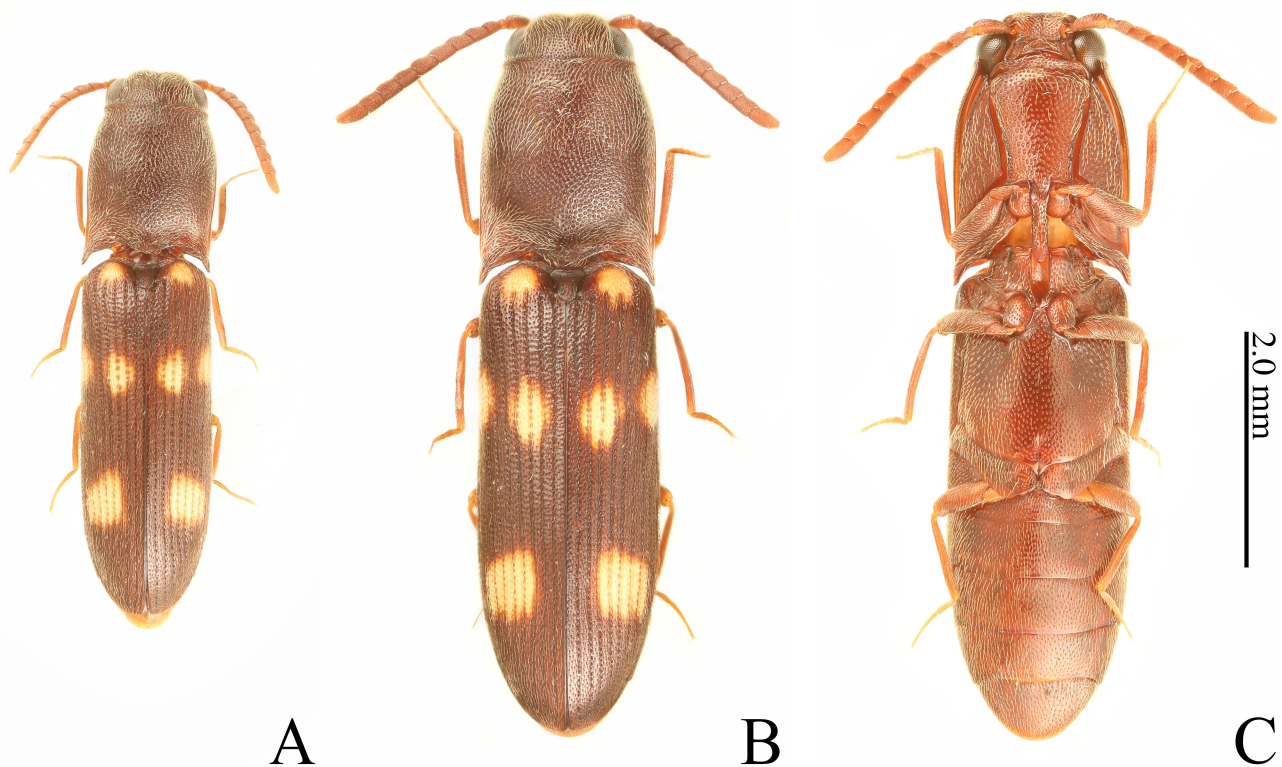


FIGURE 4. *Subprotelater miriensis* Arimoto, **sp. nov.**, male. A, B: Habitus, dorsal side; C: habitus, ventral side. A: Holotype (AA2739); B, C: paratype (AA2738).

Prothorax widened posteriad on anterior half, slightly narrowed on posterior half ahead of posterior angles (Fig. 4A), widest on its half-length or across posterior lateral apices, broadly rounded laterally on posterior 2/3. Antennal grooves between pronotum and hypomeron deep and opened anteriorly, not reaching posterior lateral apices of prothorax, visible in lateral view (Fig. 5D); sides of antennal grooves carinate. Pronotum sub-hexagonal, 1.3 × longer than wide, roundly convex but weakly constricted posterior to anterior edge (Fig. 4A, B), tallest around the center (Fig. 5D), with median longitudinal depression posteriorly; each lateral carina extending from posterior angles along antennal grooves (Fig. 5D: black arrow), not reaching anterior angles; anterior angles acute (Fig. 5A); anterior edge straight in dorsal view (Fig. 5A); posterior angles extending posteriad, acute, with median longitudinal carina vestigial; posterior edge without sublateral incision near each hind angle, lobated and protruding medially. Hypomeron depressed for reception of pro-femur and tibia, carinate behind the depression; anterior angle sharply pointed (Fig. 5J: white arrow); posterior edge broadly rounded mesally and weakly emarginate near distal posterior angle; mesal posterior angle obtuse, not protruding (Fig. 5J: black arrow). Pronotosternal sutures (Fig. 4C) deeply grooved to receive pro-tarsi; tarsal groove opened posteriorly and connected to hypomeron depression for reception of pro-femur and tibia (Fig. 5J), becoming shallower anteriorly, not reaching anterior edges of hypomeron and prosternum. Prosternum: anterior edge carinate, roundly projecting medially, depressed posterior to prosternal

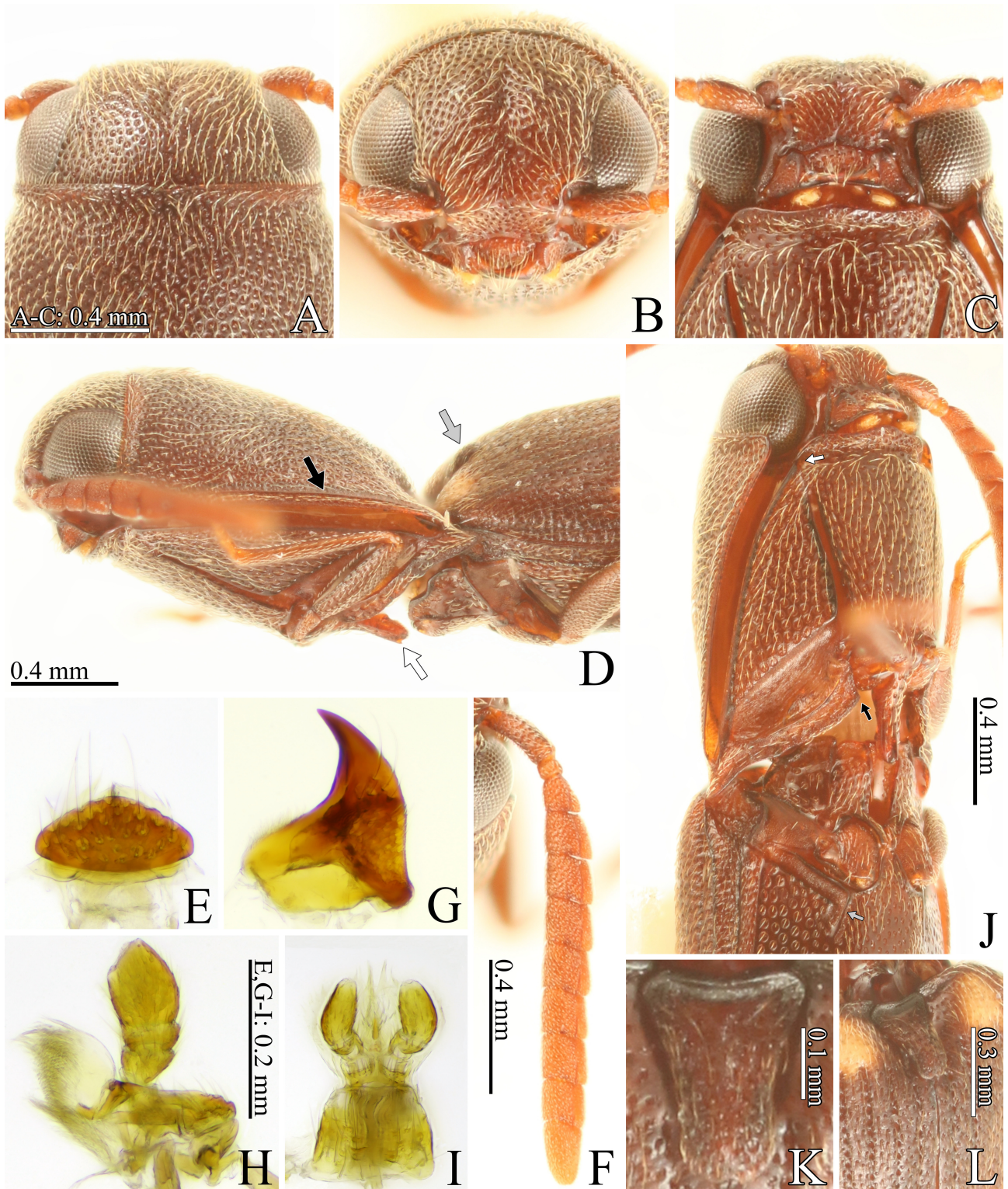


FIGURE 5. *Subprotelater miriensis* Arimoto, **sp. nov.**, holotype, male (AA2739). A: Head, dorsal view; B: head, anterior view; C: head, anteroventral view; D: head, prothorax and mesothorax, lateral view (black arrow: lateral carina along antennal groove, white arrow: pointed subapical tooth, grey arrow: posterior part of scutellar shield visible); E: labrum; F: right antenna; G: right mandible; H: right maxilla; I: labium; J: prothorax and mesothorax, ventrolateral view (white arrow: anterior angle of hypomeron sharply pointed, black arrow: mesal posterior angle of hypomeron not protruding, gray arrow: metasternum carinate ahead of depression for reception of mid-tibia and ventrad of depression for reception of mid-tarsi); K: scutellar shield; L: scutellum and elytra, dorsolateral view.

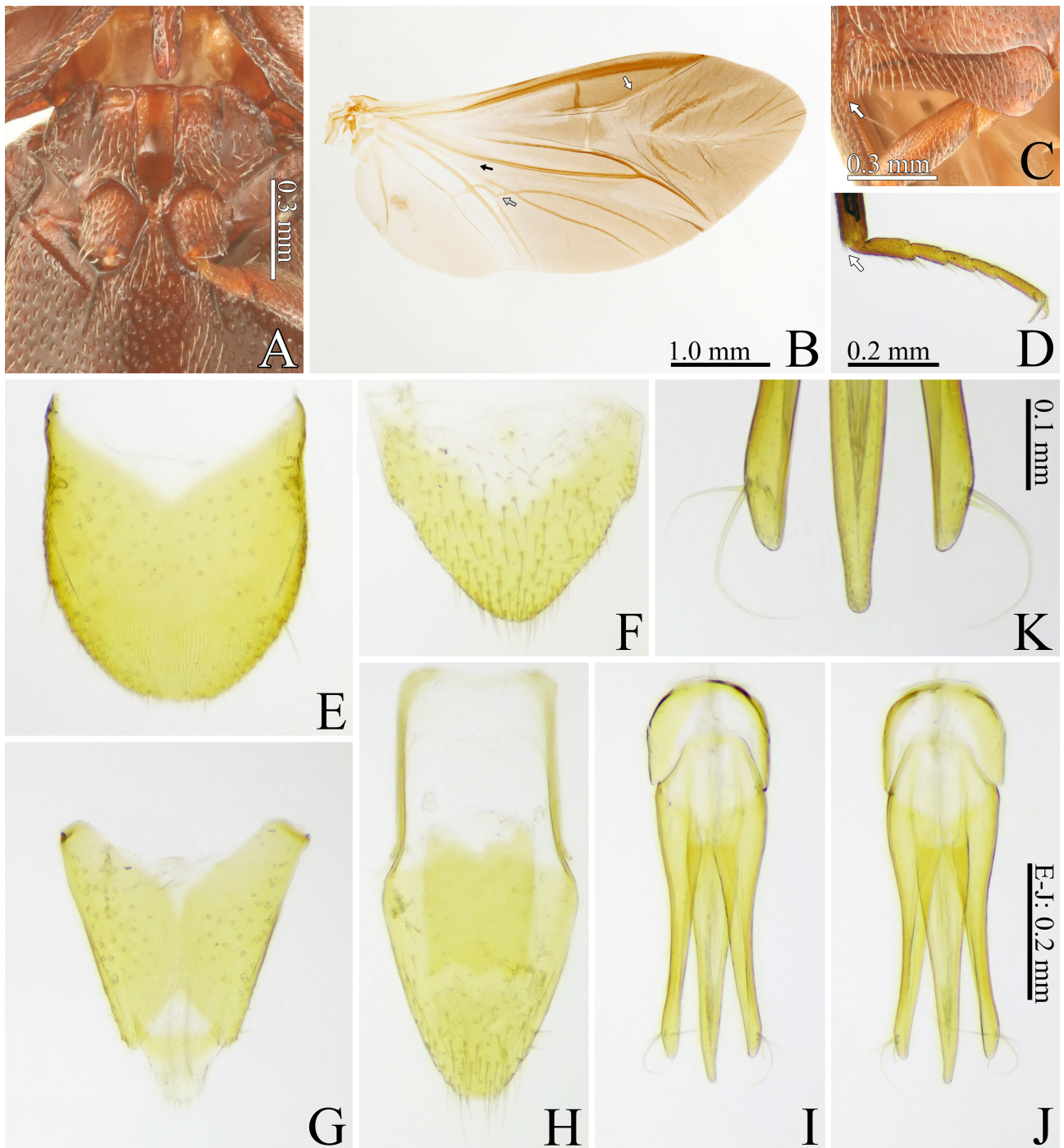


FIGURE 6. *Subprotelater miriensis* Arimoto, **sp. nov.**, male. A: Mesothorax and metathorax, ventral side; B: right hind wing (white arrow: vein RA_{3+4} vestigial, black arrow: mediomedial cross-vein between MP_{1+2} and MP_{3+4} vestigial, gray arrow: mediocubital cross-vein between MP_{3+4} and CuA_2 not complete); C: metacoxal plate (arrow: lateral posterior angle acute); D: right mid tarsus, lateral side (arrow: tibiae with a pair of simple spurs); E: tergite VIII; F: sternite VIII; G: tergites IX–X; H: sternite IX; I: aedeagus, dorsal side; J: aedeagus, ventral side; K: apical part of aedeagus, dorsal view. A, C–K: Holotype (AA2739); B: paratype (AA2741).

lobe; prosternal lobe short, not reaching the level of anterior edge of prothorax (Fig. 5D). Prosternal process 2.0–2.3 × longer than procoxal cavity length, depressed between procoxae, strongly curved dorsad behind procoxae (Fig. 5D); dorsal margin broadly rounded but with shallow concave medially in lateral view (Fig. 5D); ventral lobe almost parallel sided and gradually narrowed near apex in ventral view, with median longitudinal carina on posterior

1/3 (Fig. 4C); the carina forming pointed subapical tooth (Fig. 5D: white arrow); ventral margin rounded inward anteriorly and straight posteriorly in lateral view (Fig. 5D); ventral apex reaching dorsal apex; apex rounded in ventral and lateral views (Figs. 4C, 5D). Scutellar shield distinctly inclined anterior-downwards but posterior part parallel to elytral surface (Fig. 4A, B), tongue-shaped in anterodorsal view (Fig. 5K), narrowed posteriorly but almost parallel-sided posteriorly, 1.1–1.3 × longer than wide, convex (Fig. 5L); anterior part strongly protruding anteriorly (Figs. 4A, 5L); posterior part visible in lateral view (Fig. 5D: gray arrow); anterior angles rounded; anterior edge weakly and widely emarginate from anterior view; apex rounded or narrowly emarginate apically. Mesosternum (Fig. 6A): anterior edge straight but anterior edge of mesosternal cavity weakly protruding, lobate on each side; mesosternal cavity floor without median band of setae; mesosternal cavity almost parallel-sided anteriorly in ventral view; borders of mesosternal cavity in lateral view rounded anteriorly, straight medially and then curved ventrad obtusely (Fig. 5D); mesosternal process between mesocoxae lower than mesocoxae, not visible in lateral view (Fig. 5D); posterior edge 0.15–0.2 × wider than total width of mesosternum, almost straight (Fig. 6A); mesosternum and metasternum connate medially (Fig. 6A). Mesepisternum excavate anteriorly (Fig. 6A). Mesepimeron depressed for reception of mid-femur (Fig. 5J). Mesocoxal cavity closed to mesepisternum by mesosternum and mesepimeron (Fig. 5J). Elytron 5.2–5.45 × longer than wide, 2.0–2.2 × longer than pronotal length, parallel-sided but narrowed from posterior 1/3, rounded apically, broadly convex but plane medially (Fig. 4A), with striae. Elytral apices not meeting at midline (Fig. 4A, B). Hind wings (Fig. 6B) fully developed, without veins CuA_1 and CuA_{3+4} ; RA_{3+4} vestigial (Fig. 6B: white arrow); r4 translucent; mediomedial-cross vein between MP_{1+2} and MP_{3+4} vestigial (Fig. 6B: black arrow); mediocubital cross-vein between MP_{3+4} and CuA_2 anteriorly to contact point between MP_3 and MP_4 , not complete (Fig. 6B: grey arrow); AA3 located at contact point between CuA_2 and CAS; radial cell 3.7–4.2 × longer than wide. Metepisternum narrower than width of elytral epipleuron (Fig. 5J). Metasternum depressed for reception of mid-tibia and tarsi, carinate ahead of depression for reception of mid-tibia and ventrad of depression for reception of mid-tarsi (Fig. 5J: grey arrow), sulcate medially and ahead of metacoxal cavities (Fig. 4C). Metacoxal plate narrowed medially; lateral edge distinctly longer than width of metepisternum; lateral anterior angle rounded; lateral posterior angle broadly pointed (Fig. 6C: arrow). Tibiae with a pair of simple spurs (Fig. 6D: arrow); relative tarsomere lengths: $IV < III < II < V < I$ (Fig. 6D); tarsi and claws simple.

Abdomen. Ventrite V curved triangular, rounded apically (Fig. 4C), 0.55–0.6 × longer than wide. Tergites and sternites VIII–X yellow. Tergite VIII (Fig. 6E) longer than wide, almost parallel-sided basally but weakly sinuate, broadly rounded apically. Sternite VIII (Fig. 6F) triangular, abruptly narrowed at its half-length, shorter than wide; apex rounded. Tergite IX (Fig. 6G) trapezoidal; anterior edge widely emarginate; posterior median notch moderate (0.1–0.15 × total length of tergite IX). Tergite X (Fig. 6G) curved triangular but lateral edges sinuate in holotype, widely emarginate anteriorly, rounded apically, 0.9–1.2 × longer than wide, 0.4–0.45 × length of tergite IX. Sternite IX (Fig. 6H) parallel-sided on anterior 2/5, expanded just behind anterior half, and then roundly converging posteriorly. Aedeagus (Fig. 6I, J) yellow, elongate. Phallobase 0.25–0.3 × total length of aedeagus, 0.9–0.95 × longer than wide. Median lobe gradually tapering to apex, exceeding apices of parameres by its apex; basal struts 0.3 × total length of median lobe. Parameres separated ventrally; apical parts without lateral subapical barbs, tapering to apex, each with less than two long setae dorsally and less than two long setae ventrally.

Female. Unknown.

Etymology. The specific epithet derives from Miri, the type locality.

Distribution. Malaysia (Borneo).

Ecology. This species may be observed year-round in lowland rainforests, with specimens collected in February, May, August, and December. All specimens were captured using light traps set on trees during the night.

Discussion

Subprotelater species typically feature several yellowish spots on their black to brown elytra. Species with five spots on each elytron include *S. bakeri* and *S. hisamatsui* (Fleutiaux, 1916; Nakane, 1987a), while species with four spots include *S. lambirensis*, *S. miriensis*, *S. guttatus*, and *S. williamsi* (Fleutiaux, 1919; Van Zwaluwenberg, 1941; this study). *Subprotelater japonicus* is characterized by three spots (Nakane, 1991). Among the species with four spots, *S. lambirensis* and *S. guttatus* share similar coloration (black body, black antennae with red basal antennomeres, and red legs with femurs more or less black), but they can be distinguished by their punctures: *S. lambirensis*

has small punctures with interspaces generally larger than the puncture diameter, while *S. guttatus* features large, umbilicate punctures on the pronotum and very tight, large punctures on the prosternum and hypomeron (Fleutiaux, 1919). Additionally, the metepisternum width differentiates them: in *S. lambirensis*, it is narrower than the width of the elytral epipleuron, whereas in *S. guttatus*, it is equal to the width of the elytral epipleuron (Fleutiaux, 1919). *Subprotelater lambirensis* and *S. williamsi* are also similar in body color and size (length: 4.5 mm, width: 1.25 mm), but they differ in body proportions: in *S. lambirensis*, the elytron length is 2.0 times the pronotum length, whereas in *S. williamsi*, it is more than 2.0 times the pronotum length. Furthermore, the setae color differs: *S. lambirensis* has yellow brown setae on the whole body, while *S. williamsi* has black setae on the dorsal side and grayish setae on the underside of the body (Van Zwaluwenberg, 1941). *Subprotelater miriensis* is distinguished by its brown body, setting it apart from the other three black species with four spots (Fleutiaux, 1919; Van Zwaluwenberg, 1941). This species is relatively similar to *S. guttatus* in having a pronotum with large, umbilicated punctures but differs in terms of its antennal color (*S. miriensis*: orange; *S. guttatus*: black) and leg color (*S. miriensis*: orange; *S. guttatus*: reddish with black femurs) (Fleutiaux, 1919). In this paper, a key to the species of the genus is provided based on the features outlined in the original descriptions. However, given the potential for color variation, a detailed reexamination of the morphology of known species is necessary to accurately identify each species, including unidentified specimens (Lawrence *et al.*, 2000 onwards; Makihara and Ôhira, 2006), as well as any future new species.

This study reports the first recorded occurrence of *Subprotelater* species in Borneo, as well as the first instance of multiple species being found sympatrically. The two Bornean species are distinguished by differences in body proportions (PLI and EI), as well as the color of the body, antennae, and legs. Additional distinguishing features include the size of the punctures, the length of the prosternal process and basal struts of the median lobe, and the shape of the mesal posterior angle of the hypomeron, scutellar shield, and apices of the parameres. These characters are expected to be useful in the identification of other congeners as well.

Acknowledgments

Our study was conducted in accordance with the Memoranda of Understanding (MOU) signed by the Sarawak Forestry Corporation (SFC) and the Japan Research Consortium for Tropical Forests in Sarawak (JRCTS) in December 2005 and February 2021, as well as the MOU signed by the Forest Department Sarawak (FDS) and JRCTS in November 2012. The species names have been endorsed by the Premier Sarawak, the Right Honorable Datuk Patinggi Tan Sri (Dr) Abang Haji Zohari bin Tun Datuk Abang Haji Openg. We express our gratitude to the late Abang Abdul Hamid Karim (FDS) and the late Tamiji Inoue (Kyoto University), who were instrumental in conducting the Sarawak Canopy Biodiversity Project, under which some of the specimens studied here were collected. We thank Lucy Chong (SFC), Tohru Nakashizuka (Forestry and Forest Products Research Institute, Japan), and the late Kuniyasu Momose (Ehime University) for providing us with the opportunity to study insects in the areas surrounding Lambir Hills National Park. We also thank Runi Sylvester Pungga, Nafri Bin Ali, Empenit Empawi, and the staff of the Research and Development Division of FDS for their support during our specimen research, as well as Melvin Terry Gumal and Paschal Anak Dagang (SFC) for enabling us to continue our research after 2022. This study was financially supported by JST/JICA and SATREPS (JPMJSA1902).

References

- Arimoto, H. (2019) Record of *Subprotelater japonicus* in Nara City. *Sayabane*, New Series, 33, 55. [in Japanese]
- Arimoto, K. (2023) Taxonomic revision of the genus *Penia* Laporte (Coleoptera, Elateridae, Dendrometrinae) from Taiwan. *Zootaxa*, 5375 (3), 301–335.
<https://doi.org/10.11646/zootaxa.5375.3.1>
- Calder, A.A. (1996) Click beetles. Genera of the Australian Elateridae (Coleoptera). *Monographs on Invertebrate Taxonomy*, 2, 1–401.
<https://doi.org/10.1071/9780643105171>
- Cobos, A. (1959) Eucnemidae del Musée Royal du Congo Belge (Coleoptera). *Annales du Musée Royal du Congo Belge*, Serie in 8°, 73, 5–57.
- Costa, C., Lawrence, J.F. & Rosa, S.P. (2010) Elateridae Leach, 1815. In: Leschen, R.A.B., Beutel, R.G. & Lawrence, J.F. (Eds.), *Coleoptera, Beetles. Volume 2. Morphology and Systematics (Elateroidea, Bostrichiformia, Cucujiformia partim)*.

- In: Kristensen, N.P. & Beutel, R.G. (Eds.), *Handbook of Zoology, Arthropoda: Insecta*. Walter de Gruyter GmbH & Co. KG, Berlin/New York, pp. 75–103.
<https://doi.org/10.1515/9783110911213.75>
- Douglas, H.B. (2017) World reclassification of the Cardiophorinae (Coleoptera, Elateridae), based on phylogenetic analyses of morphological characters. *ZooKeys*, 655, 1–130.
<https://doi.org/10.3897/zookeys.655.11894>
- Eschscholtz, F. (1829) *Zoologischer Atlas, enthaltend Abbildungen und Beschreibungen neuer Thierarten, während des Flottcapitains von Kotzebue zweiter Reise um die Welt, auf der Russisch-Kaiserlichen Kriegsschlupp Predpriaetië in den Jahren 1823–1826. Erstes Heft*. G. Relmer, Berlin, iv + 15 pp.
- Fleming, J. (1821) Insecta. In: MacVey, N. (Ed.), *Supplement to the fourth, fifth and sixth editions of the Encyclopaedia Britannica, with preliminary dissertations on the history of science. Volume Fifth [Part 1]*. A. Constable and Company, Edinburgh, pp. 41–56, pl. 85.
- Fleutiaux, E. (1916) Melasidæ (Coléoptères) des îles Philippines récoltés par C. F. Baker. *Philippine Journal of Science*, 11, 38–398.
- Fleutiaux, E. (1919) Melasidae nouveaux (Coléoptères) récoltés par C. F. Baker. *Philippine Journal of Science*, 15, 445–450.
<https://doi.org/10.5962/bhl.part.11768>
- Fleutiaux, E. (1920) Études sur les Melasidae (Coleoptera-Serricornia). Première partie. *Annales de la Société Entomologique de Belgique*, 60, 93–104.
- Kundrata, R., Kubackzova, M., Prosvirov, A.S., Douglas, H.B., Fojtikova, A., Costa, C., Bousquet, Y., Alonso-Zarazaga, M.A. & Bouchard, P. (2019) World catalogue of the genus-group names in Elateridae (Insecta, Coleoptera). Part I: Agrypninae, Campyloxeninae, Hemipopinae, Lissominae, Oestodinae, Parablacinae, Physodactylinae, Pityobiinae, Subprotelaterinae, Tetralobinae. *ZooKeys*, 839, 83–154.
<https://doi.org/10.3897/zookeys.839.33279>
- Lawrence, J.F., Hastings, A.M., Dallwitz, M.J., Paine, T.A. & Zurcher, E.J. (2000 onwards) Elateriformia (Coleoptera). Version 12 September 2018. Available from: <http://delta-intkey.com> (accessed 23 October 2024)
- Lawrence, J.F., Zhou, Y.-L., Lemann, C., Sinclair, B., Ślipiński, A. (2021) The Hind Wing of Coleoptera (Insecta): Morphology, Nomenclature and Phylogenetic Significance. Part 1. General Discussion and Archostemata–Elateroidea. *Annales Zoologici*, 71, 421–606.
<https://doi.org/10.3161/00034541ANZ2021.71.3.001>
- Makihara, H. & Ôhira, H. (2006) Supplementary notes on the elatrid-beetles (Coleoptera, Elateriade) of the Ogasawara Islands held in the collection of the Forestry and Forest Products Research Institute (FFPRI), including a description of a new species. *Bulletin of FFPRI*, 5 (1), 93–97.
- Muona, J. (1987) The generic names of the beetle family Eucnemidae (Coleoptera). *Entomologica scandinavica*, 18, 79–92.
<https://doi.org/10.1163/187631287X00043>
- Nakane, T. (1987a) New or little-known Coleoptera from Japan and its adjacent regions. XXXIX. *The Review of Social Science*, 1 (1), 171–177.
- Nakane, T. (1987b) Notes on the Eucnemidae of Japan (Coleoptera). *Gekkan-Mushi*, 198, 7–11. [in Japanese, with English title]
- Nakane, T. (1991) Notes on some little-known beetles (Coleoptera) in Japan. 8. *Kita Kyûshû no Konchû*, 38 (2), 111–115.
- Noto, Y. (2024) Record of *Subprotelater japonicus* from Okutama Town, Tokyo Prefecture. *Gekkan-Mushi*, 638, 55 [in Japanese]
- Suzuki, W. (2002) New record of *Subprotelater hisamatsui* (Coleoptera, Elateridae) from Otouto-jima Island of the Ogasawara Island, Japan. *Elytra*, 30 (1), 190–191.
- Suzuki, W. (2003) Elaterid beetles of Tokyo, collected by Mr. K. Matsumoto. *Kanagawa-Chûhō*, 143, 21–32. [in Japanese, with English title]
- Suzuki, W. (2022) Notes on elaterid beetles from Otouto-jima Island of the Ogasawara Islands, Japan. *Sayabane*, New Series, 48, 38–40. [in Japanese, with English title]
- Suzuki, W. (2024) Notes on elaterid beetles from Ani-jima Island of the Ogasawara Islands, Japan. *Sayabane*, New Series, 54, 26–30. [in Japanese, with English title]
- Takahashi, Y. (2010) *Subprotelater japonicus* collected in Iwate Prefecture. *Gekkan-Mushi*, 467, 41. [in Japanese]
- Van Zwaluwenberg, R.H. (1941) A new Eucnemid beetle from New Caledonia. *Proceedings of the Hawaiian Entomological Society*, 11 (2), 219–220.
- Watanabe, A. (2008) A record of *Subprotelater japonicus* (Coleoptera, Elateridae, Subprotelaterinae) from Okayama Prefecture, Japan. *Gekkan-Mushi*, 445, 39–40. [in Japanese, with English title]
- Yamaji, O. (1998) Record of *Subprotelater japonicus*. *Nejirebane*, 80, 8. [in Japanese]